A 2D-3D Registration Tool Capable of Accurately Quantifying Flexion-Extension Positioning in the Cervical Spine

Devin A. Singh[1], Howard J. Ginsberg[2] and Cari M. Whyne[*,3]

[1]*Institute of Biomaterials and Biomedical Engineering (I.B.B.M.E.), University of Toronto, St. Michael's Hospital, Sunnybrook Research Institute, Canada*

[2]*Department of Surgery, Institute of Biomaterials and Biomedical Engineering (I.B.B.M.E.), University of Toronto, St. Michael's Hospital, Canada*

[3]*Department of Surgery, Institute of Biomaterials and Biomedical Engineering (I.B.B.M.E.), Institute of Medical Sciences, University of Toronto, Sunnybrook Research Institute, Canada*

Abstract: Flexion-extension x-rays are almost exclusively employed to analyze cervical spine kinematics. Yet, 2D radiographic measures of key vertebral metrics used to evaluate cervical stability are limited by x-ray source beam divergence, magnification errors and off-axis image acquisition. Three-dimensional CT images can be used to accurately measure these parameters, however flexion-extension CT scans are rarely acquired and do not provide information on the kinematics of the loaded cervical spine. This study evaluates the ability of an open source 2D-3D intensity-based image registration algorithm (xSePT) to create accurate flexion-extension 3D CT quality data from 2D flexion-extension radiographs and a single neutral 3D CT scan. Off axis 2D digitally rendered radiographs (DRRs) were generated from a set of 'gold standard' flexion-extension CT images of a single patient. The xSePT algorithm used the DRRs and a neutral CT to generate 3D flexion-extension CT images. Cervical vertebral metrics of subluxation, intervertebral disc height and interspinous process gap distance were compared between the 'gold standard' flexion-extension CT images, the 2D flexion-extension DRRs and the 3D output of the xSePT algorithm. The xSePT 2D-3D registration tool successfully aligned to the original flexion-extension CT data within 1° rotation and 0.5mm translation. The algorithm rapidly calculated values for the vertebral metrics equivalent to those based on the original flexion-extension CT data. Future evaluation of cervical pathology and kinematics under load may be possible through the application of this algorithm to generate 3D loaded flexion-extension data based on 2D standing flexion-extension x-rays and a single neutral unloaded CT scan.

Keywords: 2D-3D registration, radiograph, flexion-extension, cervical spine, kinematics.

INTRODUCTION

In assessing the stability of the cervical spine, radiography is the predominant tool owing to its simplicity, accessibility and speed. In particular, for segmental motion analysis of the cervical spine, functional flexion-extension x-rays are employed. The flexion-extension x-rays are taken laterally in order to assess abnormal motion caused by injury to the ligamentous structures of the spine when vertebral fractures do not present in neutral radiographs or computed tomography but pain is still reported by the patient. These functional radiographs can also be used to check the effect of surgical fusions at the desired level and at levels adjacent to the fusion site.

In order to evaluate cervical stability using flexion-extension radiographs many metrics including disc height, interspinous process distance, subluxation and adjacent vertebral level rotation are quantified [1-3]. These measurements require accurate landmarking of several key features such as the four corners of each vertebral body visible in the radiograph. The most common problem in assessing radiographs is the quality of the x-ray film obtained. Distortional effects caused by the divergence of the x-ray source beam lead to poor resolution radiographs on which it is difficult to accurately landmark key structures. In larger patients 50% or more of the cervical spine can be hidden on lateral x-rays by the patient's shoulders. Moreover, even if a high quality radiograph with well defined structures is obtained, measured values of translational and rotational metrics can be limited [4,5]. The apparent translation in the sagittal plane may be affected by the amount of rotation of the vertebrae in the sagittal plane or the amount of rotation about the vertical axis of the spine (presents when radiographs are not taken in a true lateral position). True distance measurements of subluxation are difficult to ascertain when the magnification of the x-ray image is unknown. These common radiographic problems complicate the assessment of cervical spine stability on flexion-extension x-rays and in some cases can lead to misdiagnosis.

Many of the issues associated with evaluating flexion-extension x-rays would be avoided if the movements of the cervical spine could be visualized in 3D. However, flexion-extension computed tomography (CT) images are rarely

*Address correspondence to this author at the Orthopaedics Biomechanics Lab., 2075 Bayview Ave, Rm UB-19, Toronto, ON, M4N 3M5, Canada; Tel: 416-480-5056; Fax: 416-480-5856;
E-mail: cari.whyne@sunnybrook.ca

1876-5327/11

taken (due to cost, limited resources and higher radiation dose) and when they are done it is with the patient in the supine position rendering an unloaded assessment of the cervical spine [6]. This unloaded motion often may not properly recreate the potential kinematic problems of the cervical spine. It is thus our objective in this study to develop a method for reconstructing 3D flexion-extension images based on a single neutral CT scan and flexion-extension radiographs. This 2D-3D registration technique will be evaluated in its ability to measure key metrics of cervical spine kinematics.

MATERIALS AND METHODS

Imaging

Neutral (C2-C7), flexion (C2-C7) and extension (C2-C5) cervical spine CT scans were retrospectively acquired from a single patient at a resolution of 0.3125 x 0.3125 x 0.625 mm^3 using a helical CT scanning protocol (140 KVP/597 mA, GE Medical Systems LightSpeed VCT). Digitally rendered radiographs (DRRs) were created from the flexion and extension CT scans using a ray casting method. All image analysis was completed using Amira Dev 5.1 (Visage Imaging GmbH, Germany). Off angle radiographs were created at a 7 degree rotation about the vertical axis of the spine. This orientation represents flexion and extension radiographs that are deviated from true lateral, a common occurrence in clinical radiographic imaging (Fig. **1**). These generated DRRs provide the 2D inputs for the 2D-3D registration. The corresponding neutral cervical spine CT was manually segmented for each individual cervical vertebra from C2 to C7 in order to provide the 3D image inputs for the 2D-3D registration.

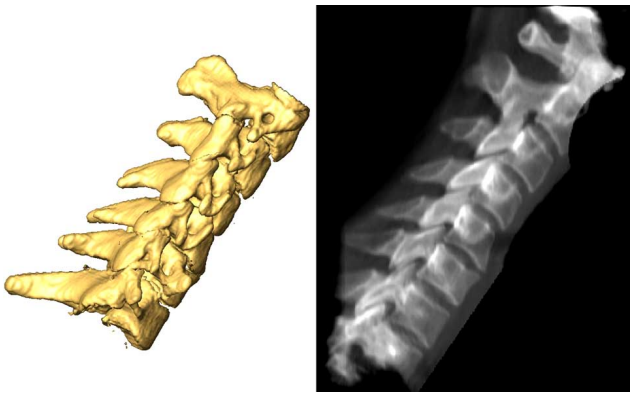

Fig. (1). Original generating CT input and digitally rendered radiograph (generated with a source to image distance of 1791 mm and a source to detector distance of 1840).

2D-3D Registration (Fig. 2)

The registration was performed using open source software xSePT developed by Steininger and Neuner [7]. This robust tool is a simple intensity based 2D-3D registration of a 3D volume (CT image) with a single 2D image (radiograph). The software treats the provided 2D x-ray as a fixed image. The 3D volume is rigidly transformed with 6 degrees of freedom about a user defined center of rotation. The registration is an iterative process with the each iteration creating a 2D projection (DRR) based on the moving 3D image. The generated projection is then matched to the fixed 2D input radiograph using histogram profile matching and the obtained transform is then applied to the input 3D image to drive the next iteration. The process is repeated for up to 1000 iterations or until convergence of the rigid transform is reached. In order to increase the precision of the algorithm the iterative process is performed on two levels with the first level using half the original xy resolution (referred to as in plane resolution for the radiograph) for both the 2D and 3D images; the second level is then carried out at the original input resolution for both images. For each of the two levels the user must also define the minimum and maximum intensity (measured in Houndsfeld units; HUs) of interest for both the fixed (radiograph) and moving (CT) histograms. This feature is essential to the 2D-3D registration process as typical 3D-3D registration is performed using volumes and not 2D projections. For this study, each isolated neutral vertebra was registered with both the flexion and extension DRRs. Refer to Appendix Table **A1** for detailed parameters used to initialize the xSePT tool in this study.

The input alignment for each isolated vertebra was initiated with the assumption that the fixed image was a true lateral radiograph. This yielded an initial 3D image placement that was 7 degrees rotated about the anatomical vertical/x axis. An artificial translation of 3.5 mm was also applied to each 3D vertebra in the coronal plane.

Validation

The quality of the 2D-3D registration was evaluated by comparing the 3D position of each vertebra prior to and following the xSePT tool to the original CT data in both flexion and extension.

Vertebral Metrics

All CTs and radiographs were landmarked at the 4 corners of the vertebral bodies when viewed in the sagittal plane and at the anterior most point of the spinous process (where it forms part of the spinal canal margin) (Fig. **3**). Vertebral subluxation, vertebral rotation and intervertebral disc height were measured for each spinal motion segment based on the work of Frobin *et al.,* [1,8] (Abobe Illustrator CS3; San Jose, CA).

Posterior vertebral subluxation was measured as the transverse distance between the inferior posterior corner of the cranial vertebra (point 3) and superior posterior corner of the caudal vertebra (point 1). Similarly, anterior subluxation was measured using the corresponding anterior corners (point 4 of cranial vertebral body and point 2 of the caudal vertebral body).

Vertebral rotation was measured as the angle formed between the determined vertebral midplanes of adjacent vertebrae. The angle is positive if the formed wedge opens anteriorly. Upon calculating the angle of vertebral rotation between adjacent vertebrae the bisectrix can be determined and placed in the disc space between the adjacent vertebrae.

The intervertebral disc height can be quantified by drawing a perpendicular line from the geometric centre of each adjacent vertebra to the bisectrix. The intervertebral disc height is the sum of the axial distances from the

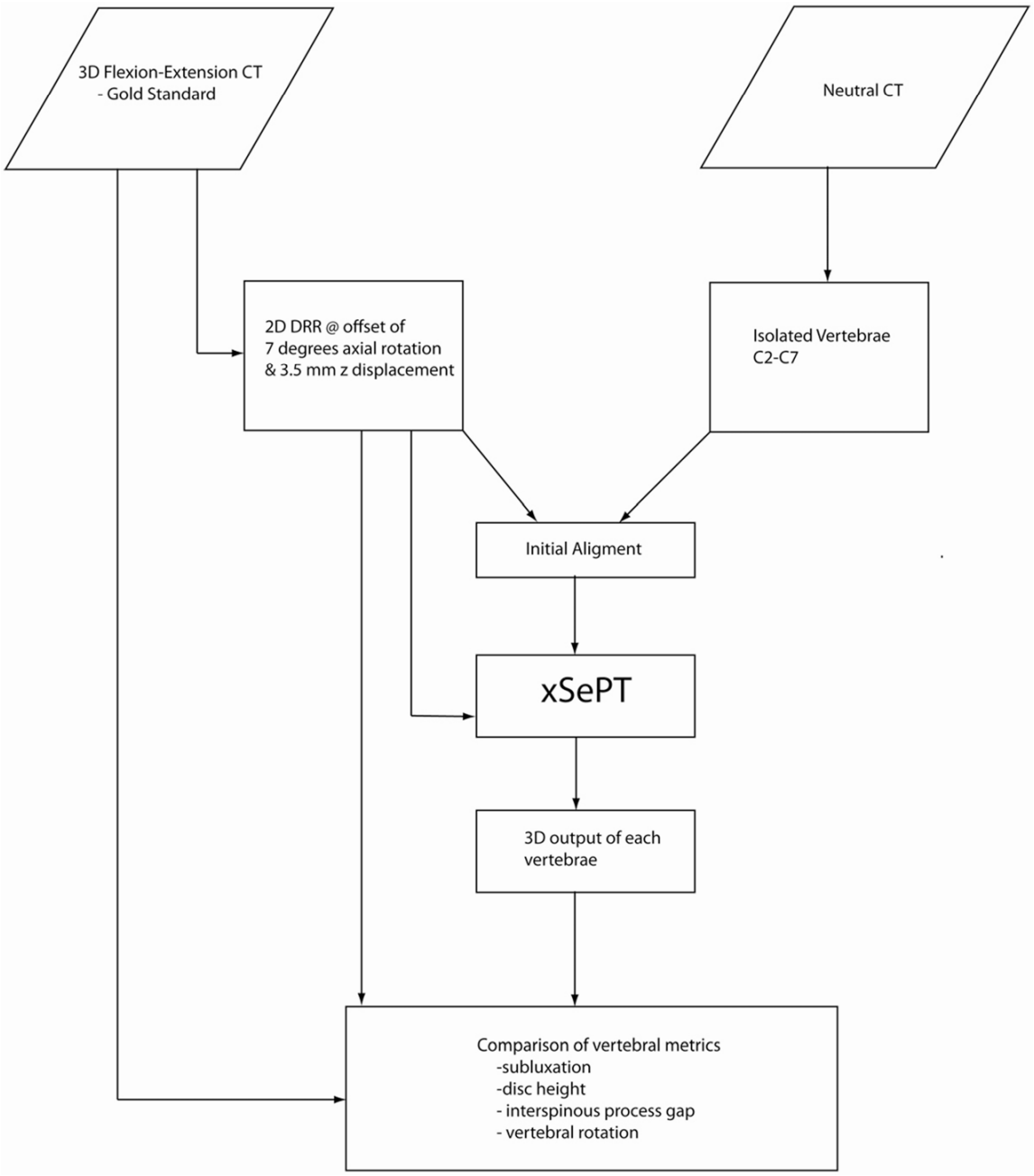

Fig. (2). Steps taken to validate xSePT 2D-3D intensity-based image registration tool using digitally rendered radiographs as the 2D input and isolated 3D vertebrae from a neutral CT. Vertebral metrics were measured in order to compare the results of the 2D-3D registration with radiographs.

bisectrix to the cortical bone margin of both the cranial and caudal vertebral body along the determined perpendicular lines.

The interspinous process distance was adapted from the work of Sobotke *et al.,* [9]. Using the more posterior of the two spinous process landmarks, the interspinous process distance is measured as the axial distance from the inferior cortical shell margin of the superior spinous process to the superior cortical shell margin of inferior spinous process.

Statistical Analysis

Pairwise t-tests were performed to make comparisons between the initial and final alignments as well as to evaluate the differences between vertebral metrics. Correlations (R^2) and mean differences between groups are reported for all tests performed on vertebral metrics with a probability level of $p<0.05$ taken as statistically significant. All statistical analysis was performed using SPSS statistical software (SPSS Inc., Chicago, IL).

RESULTS

2D-3D Registration (Tables A2 and A3)

The 2D-3D registration tool xSePT was evaluated for 6 vertebrae (C2-C7, Table **A2**) in flexion and 4 vertebrae in extension (C2-C5, Table **A3**). In flexion, the average devia-

tion with initial manual alignment was 7.01° in axial rotation and 0.5mm, 0.62mm and 3.53mm in x, y and z translation, respectively. Following the xSePT 2D-3D registration the average deviation of the final alignment was 0.43° in axial rotation and 0.37mm, 0.35mm and 0.52mm in x, y and z translation, respectively. Significant reductions in malalignment were achieved in axial rotation and z translation ($p<0.05$), corresponding to the malalignment of the generated DRRs. In extension, the average initial deviation was 6.99° in axial rotation and 0.54mm, 0.64mm and 3.59mm in x, y and z translation, respectively. Following the xSePT 2D-3D registration the average deviation of the final alignment was 0.84° in axial rotation and 0.49mm, 0.42mm and 0.48mm in translation. Similar to the flexion case, significant reductions in malalignment were achieved in axial rotation and z translation ($p<0.05$), corresponding to the malalignment of the generated DRRs (Fig. **4**).

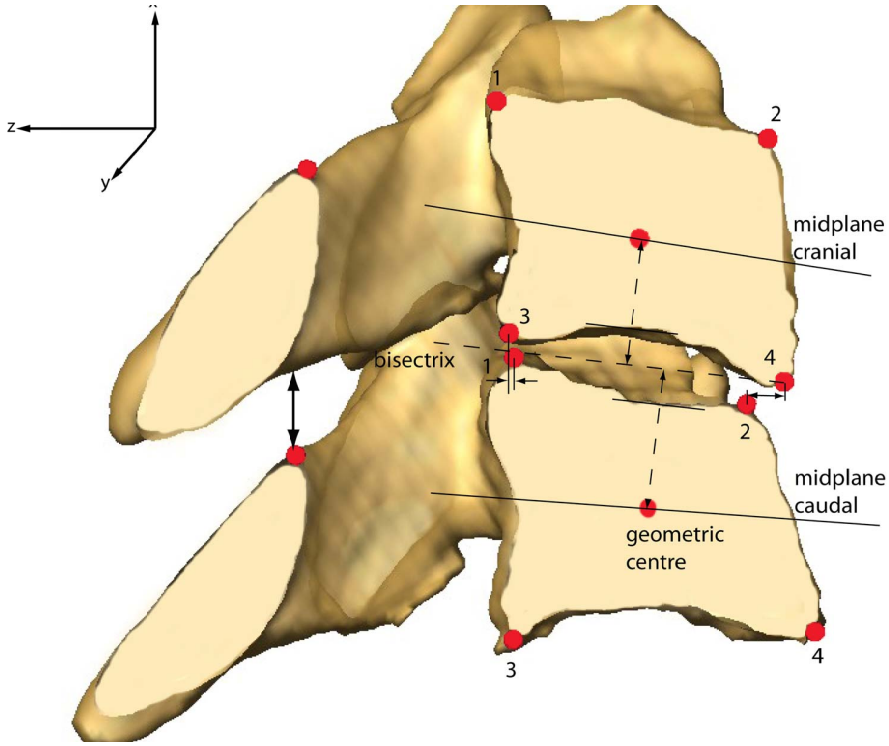

Fig. (3). Vertebral metrics as adapted from Frobin *et al.* and Sobottke *et al.* The midpoint of the two anterior vertebral corners (points 2 and 4) was used to define the midpoint of the anterior surface of the vertebral body. Likewise the two posterior corners (points 1 and 3) were used to define the midpoint of the posterior surface of the vertebral body. The line connecting the anterior and posterior midpoints defines the midplane of a given vertebra. Using all 4 corners of the vertebral body the geometric centre can also be defined.

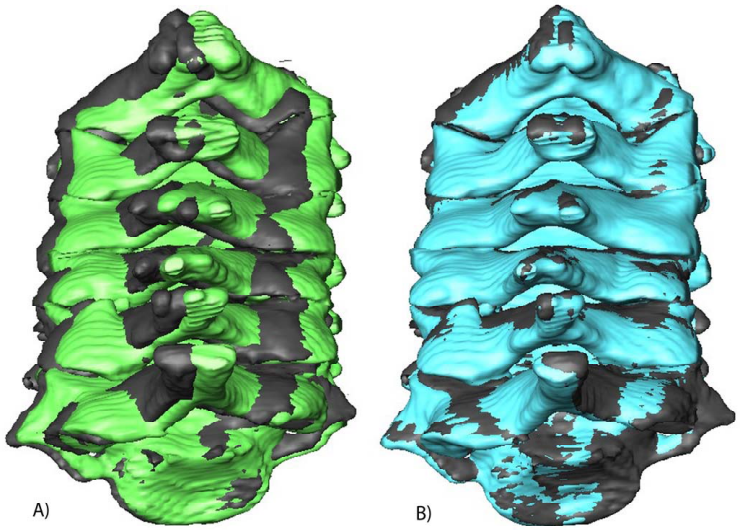

Fig. (4). A) Initial registration of cervical vertebrae assuming a true lateral radiograph (Black represents original generating CT; green represents the initial alignment). **B**) Final registration of cervical vertebrae following xSePT 2D-3D registration (Black represents original generating CT; blue represents final xSePT output.)

Vertebral Metrics (Tables A4 and A5)

Overall, the mean values for interspinous process distance, intervertebral disc height, and vertebral rotation following the xSePT 2D- 3D registration were not significantly different than the determined from the original CT. In contrast, the flexion results from the 2D DRRs were significantly different ($p<0.05$) from the original CT measurements. In extension, the difference between the 2D DRRs were significantly different from the original CT measurements only with respect to the interspinous process distance ($p<0.05$).

Specifically, in both flexion and extension, the posterior subluxation measured was found to have a higher correlation between the CT and xSePT output (flexion $R^2=0.65$; extension $R^2=0.69$) as compared to the correlation between the CT and generated DRR (flexion $R^2=0.56$; extension $R^2=0.28$). As well, the CT-xSePT mean differences were 70% lower in flexion and 47% lower in extension than the corresponding mean difference of the CT-DRR measurements. In extension, anterior vertebral subluxation yields similar results to posterior vertebral subluxation ($R^2=0.90$, 95% reduction in mean difference). In flexion, anterior vertebral subluxation also demonstrated an improvement in the correlation following xSePT ($R^2=0.88$). While the mean difference of the CT-DRR measurements in this case was less than that of the CT-xSePT measurements, the standard deviation of the CT-DRR measurements was much greater (1.1mm *vs*. 0.31mm) indicating less precision.

Intervertebral disc height in both flexion and extension demonstrated improved correlation between the CT-xSePT measurement (flexion $R^2=0.41$; extension $R^2=0.99$) when compared with the CT-DRR measurements (flexion $R^2=0.021$; extension $R^2=0.72$). Furthermore, the mean difference between the CT-xSePT measurements was reduced when compared with the CT-DRR measurements for both flexion and extension (69%, 55%, respectively).

In extension, vertebral rotation demonstrated an improved correlation between the CT-xSePT measurements ($R^2=0.96$) when compared to the CT-DRR measurements ($R^2=0.023$). In flexion, the correlation between CT-DRR measurements ($R^2=0.83$) is misleading as it represents a negative relationship between the outcome parameters. A moderate positive correlation was found for the CT-xSePT measurements ($R^2=0.52$). In both flexion and extension, the mean differences in the CT-xSePT measurements were reduced compared to the CT-DRR measurements (95% and 92% reductions respectively).

The interspinous process distance correlations between both the CT-DRR (flexion $R^2=0.83$; extension $R^2=0.96$) and the CT-xSePT (flexion $R^2=0.89$; extension $R^2=0.96$) were strong. However, in flexion, the mean difference between the CT-DRR measurements and the CT-xSePT measurements was reduced from -2.19mm to 0.71mm and in extension the corresponding mean differences were reduced from -1.16mm to -0.074mm.

Detailed quantification of the registration results and vertebral metric measurements for both flexion and extension cases can be found in Tables **A2-A5** of the appendix.

DISCUSSION

Vertebral metrics generated from 2D cervical spine x-rays are used to evaluate spinal stability. However, limitations in radiographic technology in terms of off axis image acquisition and magnification errors reduce the surgeons confidence in rendering clinical judgment based on the these values. 3D CT based measures can provide a robust evaluation of cervical spine kinematics; however flexion-extension CT scans are rarely acquired and are not in an upright loaded position. The open source xSePT 2D-3D registration tool successfully achieved an alignment to the original CT data within 1° with respect to all rotational degrees of freedom and within 0.5 mm with respect to all translational degrees of freedom in both flexion and extension. The algorithm improved the measurements of the vertebral metrics, yielding similar values to those based on the original CT data. Additionally, the tool is easy to use and analysis requires less than 1 min of processing time per vertebral level.

The inability to accurately take key measurements based on the 2D radiographs may be due to the divergence of the x-ray source beam that leads to blurring of the images, particularly at the cortical shell margins of the bone. These blurred margins affect the ability to precisely identify the edges of the bone, which may result in higher standard deviations as seen in the DRR measurements as well as variable degrees of magnification. In addition, off angle x-ray image acquisition (as simulated in this study by axial rotation) will affect 2D measurements. The ability of the xSePT method to accurately register the 2D data to high resolution 3D CT data minimizes the impact of both blurring and off angle x-ray imaging.

Currently, 3D reconstructions with biplanar radiographs (frontal and lateral) are used for the visualization of scoliotic spines, a technique known as stereoradiographic 3D reconstructions. These reconstruction techniques are divided into 2 main classes [6]. The first type requires corresponding structural landmarks visible on both radiographs with a direct linear transformation (DLT) algorithm employed to reconstruct a point in 3D using its projections on the two x-ray films [10]. While the DLT algorithm is adequate for the non-pathological vertebral bodies, the lack of stereo-corresponding points in certain vertebral regions such as the posterior arch limits the robustness of this technique [10,11]. The second, more recent technique allows for 3D reconstruction by incorporating both stereo-corresponding points (visible on both radiographs) and non stereo-corresponding points (visible in only one radiograph). This more robust technique utilizes both the DLT algorithm as well as the non stereo corresponding points (NCSP) technique to optimize the 3D reconstruction [12]. The DLT algorithm is first applied to the stereo-corresponding points and the NCSP optimizes the initial rendering based on the assumptions that: 1) the anatomical landmark to be reconstructed is situated on the line defined by the source point and the projection of the anatomical landmark on the radiograph and 2) the chosen anatomical landmark is also located on the surface of the vertebra to be reconstructed. While these techniques have reported strong results for both 3D shape reconstruction of the vertebra as well as 3D orientation one must remain aware that they are only reconstructions of a vertebra not a rigid

transformation of a pre-existing isolated 3D vertebra from CT [13]. Furthermore, it is evident that these methods are computationally intensive as well as manually laborious owing to the number of landmarks the operator needs to select. These landmark placements will also suffer from general radiographic shortcomings related to image blurring. In contrast the xSePT tool is able to register 2D to 3D data using a single planar radiographic image in conjunction with 3D histogram intensity data from an original CT image. The final 3D output is not a reconstruction but instead a rigid transformation of an original CT image yielding vertebral orientations that will not lose morphological information.

Clinically, 3D flexion and extension CT images are not frequently acquired in the cervical spine. As such our study was limited to a single data set with 6 vertebral levels visible in the flexion CT and 4 in the extension CT. The lower number of vertebrae available for analysis in extension may have limited our ability to demonstrate statistically significant differences in the extension vertebral outcome metrics.

The use of DRRs to simulate the flexion and extension radiographs was necessary to allow for validation of the registration algorithm. In the ray casting method, a simulated beam is sent from the source to the detector through each pixel on the DRR plane and the sum of all intensities encountered on this path is given as the final intensity of the DRR at that location. For this reason we were able to effectively choose threshold values for the xSePT tool registration based on each individual vertebra's CT histogram. However, the ray casting method does not effectively simulate true clinical radiographic images, as it does not account for x-ray beam divergence which skews the actual intensity values on the x-ray film. The xSePT tool is, however, equipped to handle clinical radiographs by incorporating an option to specify an intensity transfer function. The intensity transfer function allows the user to choose key structures present in both the 2D and 3D images and derive a stepwise linear relationship between the intensities of the CT and radiographic images to account for the x-ray beam divergence [14].

The xSePT open source tool has demonstrated itself to yield robust 2D to 3D registration using 3D CT data and 2D plain radiographs. While the specific 3D imaging modality (CT) required as the input for the tool provides spinal kinematic information related to the motion of the bony structures of the vertebral column, it does not visualize the behavior of the associated soft tissues. One of key motivators for acquiring loaded flexion-extension information of the cervical spine, however, is to assess the effects of motion on the soft tissue structures, particularly the spinal cord. To achieve this requires the integration of 3D soft tissue imaging data into the registration procedure. Much work has been done regarding methods for merging CT with magnetic resonance image (MRI) to yield registrations that contain both bony structure and soft tissue information [15-18]. If MRI data could be incorporated into the xSePT tool it would be a first step in obtaining a 2D-3D registration that could provide a comprehensive view of motion in the spinal column. The interpolation of soft tissue behavior requires an in depth understanding of the underlying material properties that may motivate the use of computational modeling tools, such as finite element analysis. Recent advances in MRI may obviate the need for CT imaging and allow the acquisition and integration of a single imaging modality to obtain both bone and soft tissue information [19-22]. Such 3D MRI data combined with 2D radiographs could be used as the input to the xSePT tool to yield 3D kinematic information of the bony vertebral structures as well as details of the soft tissue responses to such motion.

Overall, this study demonstrates the ability of 2D-3D registration to yield improved accuracy of important vertebral metrics utilized for clinical assessment of cervical spine stability. This method utilizes flexion extension radiographs and CT data in a neutral position which are acquired as a current standard of care in orthopaedic and neurosurgical clinical practice. Acquisition of controlled flexion-extension loaded radiographs may allow future evaluation of the xSePT registration algorithm as a tool for generating loaded 3D flexion-extension images from 2D x-ray data and a single neutral CT to facilitate the evaluation of cervical pathology and kinematics not evident in unloaded imaging.

Appendix

Table A1. Input Parameters for 2D-3D Registration Using Open Source xSePT Registration Tool. All Input Images (CT and Radiographs) were Scaled to have Intensity Values Ranging from 0 to 255 HUs

Algorithm Level	Input	Threshold Value (HUs)	
		Minimum	Maximum
Level 1	Fixed (radiograph)	176	255
	Moving (CT data)	(Median histogram intensity) - 5	255
Level 2	Fixed (radiograph)	176	255
	Moving (CT data)	Median histogram intensity	255

Table A2. Flexion 2D-3D Registration Before and after xSePT Tool (* Represents Statistically Significant Differences in the Mean Values of the Initial and Final Alignment, p<0.05)

		x Rotation (deg)*	y Rotation (deg)	z Rotation (deg)	x Translation (mm)	y Translation (mm)	z Translation (mm)*
C2	Initial	7.04	0.04	0.18	0.56	0.59	3.49
	Final	0.035	0.055	1.02	0.20	0.22	1.01
C3	Initial	7.00	0.01	0.11	0.47	0.54	3.58
	Final	0.04	0.12	0.91	0.22	0.34	0.27
C4	Initial	7.03	0.06	0.05	0.49	0.51	3.54
	Final	0.92	1.16	0.14	0.43	0.53	0.42
C5	Initial	6.99	0.01	0	0.51	0.56	3.55
	Final	1.16	0.23	0.61	0.29	0.56	0.49
C6	Initial	6.99	0	0.08	0.48	0.55	3.46
	Final	0.39	0.51	0.78	0.67	0.26	0.01
C7	Initial	6.99	0	0	0.49	0.94	3.53
	Final	0.01	1.18	0.57	0.40	0.17	0.90
Average	Initial	7.01±0.03	0.02±0.02	0.07±0.07	0.54±0.05	0.64±0.23	3.59±0.04
	Final	0.43±0.50	0.54±0.51	0.67±0.31	0.49±0.06	0.42±0.11	0.48±0.28

Table A3. Extension 2D-3D Registration before and after xSePT Tool (* Represents Statistically Significant Differences in the Mean Values of the Initial and Final Alignment, p<0.05)

		x Rotation (deg)*	y Rotation (deg)	z Rotation (deg)	x Translation (mm)	y Translation (mm)	z Translation (mm)*
C2	Initial	6.99	0	0.44	0.59	0.98	3.65
	Final	0.85	0.07	1.05	0.43	0.43	0.74
C3	Initial	6.99	0.06	0.25	0.57	0.54	3.6
	Final	1.25	0.32	0.05	0.57	0.29	0.44
C4	Initial	6.98	0.02	0.08	0.51	0.47	3.57
	Final	1.08	0.05	0.10	0.48	0.57	0.10
C5	Initial	7.00	0.02	0.11	0.49	0.57	3.55
	Final	0.16	0.36	0.34	0.49	0.41	0.65
Average	Initial	6.99±0.01	0.02±0.16	0.22±0.16	0.54±0.05	0.64±0.23	3.59±0.04
	Final	0.84±0.48	0.20±0.16	0.38±0.46	0.49±0.06	0.42±0.11	0.48±0.28

Table A4. Flexion Vertebral Metrics before and after xSePT Tool (* Represents Statistical Significant Differences in the Means of a Measured Metric or Statistically Significant Correlations at a Level of p <0.05. † Represents Negative Correlation)

	CT (mm)	2D DRR (mm)	xSePT (mm)	CT – DRR Mean Difference (mm)	CT - DRR correlation (R2)	CT - xSePT Mean Difference (mm)	CT - xSePT Correlation (R2)
Posterior Subluxation (mm)	0.78±0.42	0.31±0.20	0.65±0.41	0.47±0.59	0.56	0.14±0.26	0.65
Anterior Subluxation (mm)	1.18±0.55	1.20±1.14	1.35±0.75	-0.014±1.1	0.07	-0.17±0.31	0.88 *
Interspinous Process Distance (mm)	4.61±1.53	6.80±2.00	3.90±1.10	-2.19±0.88 *	0.83*	0.71±0.61	0.89 *
Intervertebral Disc Height (mm)	3.51±0.62	4.80±0.59	4.08±0.91	-1.29±0.92 *	0.021	-0.58±0.70	0.41
Vertebral Rotation (mm)	-4.1±1.63	1.56±1.20	-4.39±1.57	-5.66±2.77 *	0.83 (†)	0.29±1.99	0.52

Table A5. Extension Vertebral Metrics before and after xSePT Tool (* Represents Statistical Significant Differences in the Means of a Measured Metric or Statistically Significant Correlations at a Level of p <0.05)

	CT (mm)	2D DRR (mm)	xSePT (mm)	CT - DRR Mean Difference (mm)	CT - DRR correlation (R^2)	CT - xSePT Mean Difference (mm)	CT - xSePT Correlation (R^2)
Posterior Subluxation (mm)	1.01±0.52	0.24±0.10	0.60±0.17	0.77±0.48	0.28	0.41±0.23	0.69
Anterior Subluxation (mm)	1.31±0.47	0.92±0.59	1.30±0.51	0.40±1.04	0.78	0.02±0.24	0.90
Interspinous Process Distance (mm)	3.42±1.18	4.58±1.07	3.50±0.85	-1.16±0.25 *	0.96	-0.074±0.40	0.96
Intervertebral Disc Height (mm)	3.34±0.85	2.45±0.22	2.94±0.48	0.89±0.62	0.72	0.40±0.51	0.99
Vertebral Rotation (mm)	1.05±4.84	-1.37±2.64	1.24±5.36	2.42±5.15	0.023	-0.19±1.15	0.96

REFERENCES

[1] Frobin W, Leivseth G, Biggemann M, Brinckmann P. Sagittal plane segmental motion of the cervical spine. A new precision measurement protocol and normal data of healthy adults. Clin Biomech 2002; 17: 21-31.

[2] Wu S, Kuo L, Lan HH, Tsai S, Chen C, Su F. The quantitative measurements of the intervertebral angulation and translation during cervical flexion and extension. Eur Spine J 2007; 16: 1435-44.

[3] Knopp R, Parker J, Tashjian J, Ganz W. Defining radiographic criteria for flexion-extension studies of the cervical spine. Ann Emerg Med 2001; 38: 31-5.

[4] Shaffer WO, Spratt KF, Weinstein J, Lehmann TR, Goel V. The consistency and accuracy of roentgenograms for measuring sagittal translation in the lumbar vertebral motion segment: an experimental model. Spine 1990; 15: 741-50.

[5] Frobon W, Brinckmann P, Leivseth G, Biggemann M, Reikerås O. Precision measurement of segmental motion from flexion-extension radiographs of the lumbar spine. Clin Biomech 1996; 11: 547-65.

[6] Mitulescu A, Skalli W, Mitton D, De Guise JA. Three-dimensional surface rendering of scoliotic vertebrae using a non-stereo corresponding points technique. Eur Spine 2002; 11: 344-52.

[7] Steininger P, Neuner M, Schubert R. An extended ITK-based framework for intensity-based 2D/3D-registration. Technical Report. Institute of Bioedical Image analysis, University for Health Sciences, Medical Informatics and Technology 2009, available at: (http://ibia.umit.at/ResearchGroup/Phil/web/Simple2D3DRegistrationFramework.html)

[8] Frobin W, Leivseth G, Boggemann M, Brinckmann P. Vertebral height, disc height, posteroanterior displacement and dens-atlas gap in the cervical spine: precision measurement protocol and normal data. Clin Biomech 2002; 17: 423-31.

[9] Sobottke R, Koy T, Röllinghoff M, *et al.* Computed tomography measurements of the lumbar spinous process and interspinous process space. Surg Radiol Anat 2010; 32: 731-8.

[10] André B, Dansereau J, Labelle H. Effect of radiographic landmark identification errors on the accuracy of three-dimensional reconstruction of the lumbar spine. Med Biol Eng Comput 1992; 30: 569-75.

[11] Aubin CE, Dansereau J, Parent F, Labelle H, De Guise JA. Morphometric evaluations of personalised 3D reconstructions and geometric models of the human spine. Med Biol Eng Comput 1997; 35: 611-8.

[12] Mitton D, Landry C, Véron S, Skalli W, Lavaste F, De Guise JA. A 3D reconstruction method from biplanar radiography using non stereocorresponding points and elastic deformable meshes. Med Biol Eng Comput 2000; 38: 133-9

[13] Dumas R, Le Bras A, Champain N, *et al.* Validation of the relative 3D orientation of vertebrae reconstructed by bi-planar radiography. Med Eng Phys 2004; 26: 415-22.

[14] Steininger P, Neuner M, Birkfellner W, *et al.* An ITK-based implementation of the stochastic rank correlation (SRC) Metric. Insight Journal 2010: July-December. Available at:(http://www.insight-journal.org/browse/publication/776)

[15] Chen Y and Wang M. Three-dimensional reconstruction and fusion for multi-modality spinal images. Comput Med Imaging Graph 2004; 28: 21-31.

[16] Lu X, Zhang S, Su H, Chen Y. Mutual information-based multimodal image registration using a novel joint histogram estimation, Comput Med Imaging Graph 2008; 32: 202-9.

[17] Eldib A, Yamany S, Farag A. Multi-modal medical volumes fusion by surface matching. In: Taylor C, Colchester A, Eds. MICCAI'99, LNCS 1679, Heidelberg, Berlin: Springer-Verlag 1999; pp. 672-9.

[18] Piella G, Heijmans H. Multiresolution image fusion guided by multimodal segmentation. Proceedings of ACIVS 2002 (Advanced Concepts for Intelligent Vision Systems), Ghent, Belgium. 2002.

[19] Blamire AM. The technology of MRI – the next 10 years. Br. J. Radiol 2008; 81: 601-17.

[20] Idiyatullin D, Corum C, Park J-Y, Garwood M. Fast and quiet MRI using a swept radiofrequency. J Magn Reson 2006; 181: 342-9.

[21] Horch RA, Nyman JS, Gochberg DF, Dortch RD, Does MD. Characterization of ^{1}H NMR signal in human cortical bone for magnetic resonance imaging. Magn Reson Med 2010; 64: 680-7.

[22] Techawiboonwong A, Song HK, Leonard MB, Wehrli FW. Cortical bone water: *In vivo* quantification with ultrashort echo-time MR imaging. Radiology 2008; 248: 824-33.

Received: November 04, 2010 Revised: December 28, 2010 Accepted: February 28, 2011